# ASSESSMENT AND COMPARISON OF REGISTRATION ALGORITHMS BETWEEN AERIAL IMAGES AND LASER POINT CLOUDS

A. Pothou[a,*], S. Karamitsos[b], Prof. A. Georgopoulos[a], I. Kotsis[b]

[a] Laboratory of Photogrammetry - (apothou, drag)@central.ntua.gr
[b] Laboratory of Higher Geodesy - karamits@ central.ntua.gr, jkotsis@survey.ntua.gr
School of Rural & Surveying Engineering, National Technical University of Athens

**Commission I, WG I/2**

**KEY WORDS:** Registration, LiDAR, Photogrammetry, Fusion, Laser Point Cloud, DEM Matching

**ABSTRACT:**

Photogrammetry, has been providing accurate coordinate measurements through the stereoscopic method for many years. LiDAR on the other hand, is becoming the prime method for large-scale acquisition of elevation data due to its capability of directly measuring 3D coordinates of a huge number of points. LiDAR can provide measurements in areas where traditional photogrammetric techniques encounter problems mainly due to occlusions or shadows. However LiDAR has also its limitations due to its inability of thematic information recording. The aim of this research is the optimum exploitation of both these elevation data sources. Usually this process is referred to as fusion of two datasets and exploits the advantages of both sources. The prerequisite step for the fusion of the two datasets is the co-registration.
This paper describes a co-registration procedure, between the two datasets, that takes place through a 3D transformation. The performance of the algorithm A, which was presented in an earlier publication by the authors, and also an extended algorithm B based on the inclusion of the 7 transformation parameters, during the whole registration procedure, have been presented. Both algorithms developed based on the minimization of the distances between points of one surface to surface patches of the other surface, parallel to the corresponding surface normals. A comparison has also been performed between the results of the algorithms developed, in order to assess the geometric stability of the transformations, the analysis of the results, the effects on the registration and the accuracy of the derived parameters through stand-alone macros. Due to improved geometry of extended algorithm B an increased performance was expected. In fact the algorithm B converges 50% faster than the algorithm A. To support these tests a block of aerial images and a one month apart 3D laser point cloud were collected.

## 1. INTRODUCTION

There are several technologies, nowadays, to obtain 3D information of the Earth's surface. Photogrammetry, on one hand, for many years has been providing accurate coordinate measurements through the stereoscopic method. This traditional method, has its exclusive advantages but also some disadvantages. The second one, LiDAR (Light Detection And Ranging, also known as Airborne Laser Scanning - ALS) is a newer technology, highly automated, still improving and with excellent vertical accuracy of points measurements. Although LiDAR has many benefits, it still has an inherent inability to record thematic information. Moreover, issues such as filtering of some undesired information and discrimination between terrain features and extruding man-made and other objects are still under investigation by many researchers. However this method is becoming the prime method for large-scale acquisition of elevation data due to its capability to directly measure 3D coordinates of a huge number of points. Several countries are currently using LiDAR for creating or updating dense digital elevation models (DEMs). LiDAR can provide measurements in areas where traditional photogrammetric techniques encounter problems due to occlusions or shadows. Also LiDAR's satisfying capability to penetrate canopies gives it an important advantage in comparison to photogrammetry. Photogrammetry, however, can provide geometrically accurate features such as e.g. edges of buildings which LiDAR cannot.
Therefore, the two technologies if used together work complementarily to each other to extend the range and the utilization of the information gathered due to the data fusion that can occur. This fusion task of both sets of data should provide an improved digital elevation model (DEM). This approach has been suggested recently by many researchers (Ackermann, 1999, Baltsavias, 1999, Csatho et al., 1999, Toth and Grejner-Brzezinska, 1999, Vosselman 1999, Postolov et al., 1999, Habib and Schenk, 1999). For the fusion to occur, co-registration of the two datasets is required. Only then can the detected on the aerial images 3D features, be integrated with the digital elevation model (DEM) provided from LiDAR. However, the main questions that rise are: How could a matching procedure between irregularly spaced points be applied? How could two point sets, which are irregularly distributed hence lacking one-to-one correlation of their points, be co-registered? Registration is not a problem specific to the laser scanner domain. Registration between point clouds derived from different sources and by different methods which represent the same object surface, should be defined as a surface matching problem. Eventually the registration between 3D sets of points is assumed and investigated as a DEM matching problem.
The ICP (Iterative Closest Point) algorithm (Besl and McKay 1992) was considered one of the most popular methods for many years. However, the ICP algorithm assumes that one point set is a subset of the other which is not applicable between Lidar and photogrammetric points where no conjugate points are exist. The DEM matching, using DEM as control information in order to solve the absolute orientation of models was first proposed by Ebner and Mueller (1986) and by Ebner

* Corresponding author

and Strunz (1988) and many researchers have used it and its improvements in practice since. In the research by Schenk et al. (2000), two main mathematical methods, which are assumed suitable to find optimal transformation parameters between two sets and without identical points, are presented. These mathematical methods are based: a) on the minimization of the distance (min D) between a point of one surface and a surface patch of the other surface, and b) on the minimization of the remaining difference along the Z-axis (min Z), respectively. Habib and Schenk (1999) have implemented the first mathematical method minimizing the distance (min D) between a point of one surface parallel to the normal of a surface patch of the other surface. A voting scheme, based on the Modified Hough Transformation, to analyze the parameter space was proposed. Postolov et al. (1999) implemented the second mathematical method minimizing the remaining differences along the Z-axis (min Z) of one of the reference systems and dividing the 3D transformation into a sequence of planimetry and elevation transformations.

Integration of point clouds, through a DEM matching, has also been mentioned in researches regarding registration of sequential laser strips. In order to provide a high density laser point dataset over an extended surface area, many parallel overlapping laser strips are needed. This registration of sequential laser strips has been a major area of research (Burman, 2000, Maas, 2000). Gruen (1985a) first regarded the issue of the surface patch matching as a straight extension of Least Squares Matching (LSM). Gruen and Akca (2004), Akca (2004) extended the Least Square Matching theory to Least Squares 3D Surface Matching (LS3D), estimating the 3D transformation parameters between two or more arbitrarily oriented 3D surface patches.

In the present research a comparison and assessment of two supplementary registration algorithms (A and B) between aerial images and laser point clouds was performed by establishing stand-alone macros. The algorithm A has been presented (Pothou et al., 2006a), based on Schenk theory, minimizing the distances between points of one surface and surface patches of the other surface, parallel to the corresponding surface normals. It took place through a 3D transformation assessing it under real conditions and with real data. The problem was defined as surface matching problem due to the use of different methods and devices from which the 3D point sets were derived. The mathematical method, which is based on the minimization of the distances, presents better adjustment when the surface is derived from a man-made area (urban). In this type of areas one can find a variety of surface orientations of planar surfaces including vertical surfaces. The performance of algorithm A was evaluated on the test data used in order to create the local surface patches. The surface by which the local surface patches are created was referred to as control surface. Control surface is usually assumed as the surface derived by photogrammetric means. To check the algorithm, a few tests inverting the task of the surfaces were evaluated. In those tests the LiDAR points were used as control reference system and the surface generated by photogrammetric means was registered.

Moreover, special emphasis was given on the processing steps of datasets. The processing steps of datasets included: a) a variance of levels of densification of data points, through a linear interpolation, so that a denser triangulation was produced and b) a small movement (1mm) of the points presenting the lower z value (e.g. the lower edge between the two edges of a wall on a building) in order to overcome the 2D Delaunay's algorithm limitation. The transformation parameters between the two surfaces, both of which contain irregularly distributed points, were determined without requiring the surfaces to be interpolated to a regular grid. Instead a TIN model was produced.

The parameters represent a 3D transformation and include scale, translations and rotations. Parameters are estimated through a Gauss Markov model.

An extension of the algorithm A to algorithm B is introduced in this paper. Algorithm B is based on the inclusion of 7 transformation parameters, during the whole iterative Least Square procedure. The algorithms were compared and assessed minimizing the distance perpendicular to the surface patches.

The test data, which will be described, include a 3D laser point cloud and a block of aerial images collected within a time interval of one month. A 3D point set was derived by photogrammetric means from the aerial images. The proposed implementation of the algorithms for the DEM matching, the mathematical models, the experimental results as well as the analysis of the results and the effects on registration using stereo points and laser point cloud are described.

## 2. DATA DESCRIPTION

In 2004 the EuroSDR (European Spatial Data Research) Building Extraction Comparison Workshop took place (Kaartinen et al., 2005). Data were provided by the Finnish Geodetic Institute of a test area called Espoonlahti and is located in Espoo, a city about 15km west of Helsinki (Finland) with high-rise buildings and terraced houses. Additional details can be found in Pothou et al., 2006a. Two point datasets were used.

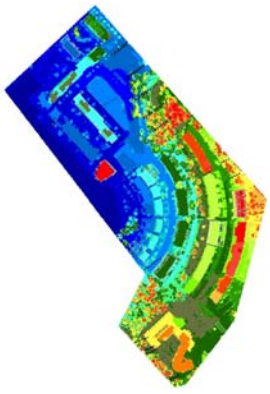

**Figure 1**. Espoolahti test site – LiDAR data

**Figure 2**. Espoolahti test site – Aerial Image

One captured by a Toposys Falcon Laser scanner (Figure 1) and the other produced by photogrammetric means from a stereo model of aerial images (Figure 2) as a full restitution of the same area and also in the same time period in order to avoid capturing changes that may have happened in the area (e.g. buildings, environmental conditions).

For this research, a full restitution including segments of the buildings, points on the roofs and points on the ground, where manually measured on a Z/I ImageStation DPW. The exterior orientation parameters of the aerial images were determined by a GPS/INS assisted aerotriangulation. The uncertainty of the exterior orientation parameters is considered better than 5cm and $30^{cc}$ for the translations and rotations, respectively. The accuracy of the measurements should also be of the same order, therefore, in the projects standard deviation of 5cm was used taking into account the specific conditions during the restitution (visual quality of the target).

### 2.1 Filtering of LiDAR points

LiDAR points captured by a Toposys Falcon Laser scanner have a high density (10-20 points/$m^2$). Many algorithms have been developed for filtering the LiDAR points (Kraus and Pfeifer, 1998, Axelsson, 1999 and 2000, Vosselman, 2000). Filtering is typically referred to the determination of the terrain. In our research a filter performed in order to eliminate the vegetation around buildings is based on the algorithm presented by Paska and Toth (2003). The spatial behavior of the LiDAR points is analyzed through a moving window-based algorithm. A window is moved over the entire dataset and in each window basic statistical parameters are calculated; such as standard deviation, maximum gradient among points, and the difference between the maximum and minimum elevations.

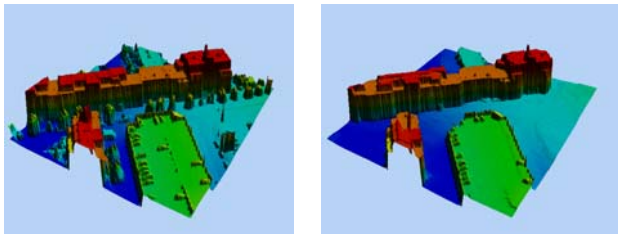

**Figure 3.** Morphological opening on vegetation: original dataset (left), opening applied (right)

The detection of areas with given height jumps, i.e. the difference between the maximum and minimum elevations in a window is higher than a given value, can be used for identifying breaklines (including natural breaklines), edges of buildings and local height variations from the point cloud. Vegetation removing is based on morphological filtering. The elevation of the point on which the kernel is centered is replaced with the minimum or maximum elevation inside the window. The opening (dilation after erosion) is typically used for terrain extraction. This method provides an easy way to eliminate single trees. The choice of the window size is crucial. To safely remove vegetation, at least one hit from the ground must exist in each window in vegetated areas. Simple opening will not filter out buildings, which are bigger than the window size. In this research, filtering took place before co-registration. The area depicted in Figure 3, is a small part of region depicted in Figure 2, in Espoolahti, which was used for testing and evaluating of both algorithms. In this part the results of the morphological filtering are clearly visible. However, there are some 'fuzzy' areas, as the one highlighted in Figure 5, where manually filtering process would be necessary.

## 3. IMPLEMENTATION OF THE REGISTRATION ALGORITHMS

As already mentioned, the first dataset P={$p_1$, $p_2$, …, $p_n$} was derived from a photogrammetric restitution and includes elevation points, segments and breaklines. The second dataset Q={$q_1$,$q_2$,…,$q_m$} includes the laser point set. The points in the two sets were irregularly distributed, while the point density was different in each of them (n≠m), hence there are no pairs of conjugate points between the two sets. Both datasets were treated as point data (x,y,z) (Morgan and Habib, 2002, Baltsavias, 1999).

The ultimate goal is to find optimal transformation parameters between the surfaces P and Q. The observation equations based on the difference in the distances between points of one surface and surface patches of the other surface, parallel to the corresponding surface normals, were used (Schenk et al., 2000). This mathematical method is assumed suitable in surfaces with a variety of orientations, including vertical surfaces with high gradients as is the present data. The transformation parameters between the surfaces, both of which contain irregularly distributed points, were determined without being interpolated to a regular raster grid. Instead a TIN model was produced (Habib and Schenk, 1999). More details can be found in the next subsection.

Initially one of the two datasets is considered as reference. Pixel size of images is equal to 14 μm, therefore measurements in a digital photogrammetric workstation were assumed to have high reliability. Manual planimetry and vertical measurements seem to be close to the ground truth, consequently surface generated by photogrammetric means P was chosen as the control reference system while the surface generated by the laser scanning Q was registered allowing the surfaces to be transformed to a common coordinate system (Figure 4).

The 2D Delaunay triangulation has been mostly used for 2.5D surfaces, whose analytic function is described in the explicit form z = f(x,y). This formulation has several problems in the matching of solid 3D surfaces due to the fact that these points are structured to shape triangles within the 2D convex hull of the data. Only two sets of coordinates, namely, x and y, are used for this purpose and the spatial relationships among points are limited to their projected distances on the x-y plane (Morgan and Habib, 2001, Balis et al., 2003). As a result, two points with the same x and y coordinates but with different z coordinate are not able to take part in a 2D Delaunay triangulation successfully. Thus, the triangles required to represent the 3D digital surface model fail to be constructed. Therefore, the above is a considerable limitation of using 2D Delaunay for city models generation (man-made constructions, building walls). Morgan and Habib (2001) have proposed a region-growing algorithm to overcome this limitation. In Pothou et al. 2006a a small movement (1mm) of the points presenting the lower z value (e.g. the lower edge between the two edges of a wall on a building) in order to overcome the 2D Delaunay's algorithm limitation was assumed adequate.

### 3.1 Mathematical Model of Algorithm A

The object is to transform two datasets into a common system. Assuming both the datasets as point clouds P ($x_{pi}$, $y_{pi}$, $z_{pi}$) ($p_i$=1,…, n) and Q ($x_{qi}$, $y_{qi}$, $z_{qi}$) ($q_i$=1,…, m) as produced by different methods, they must be transformed into a common system. A 7-parameter transformation is used minimizing the distance between a point of Q surface and a TIN surface patch of P surface. In Equation 1, points of surface Q are transformed into the system P of the control surface.

$$\begin{bmatrix} x_p \\ y_p \\ z_p \end{bmatrix} = c \cdot R \cdot \begin{bmatrix} x_q \\ y_q \\ z_q \end{bmatrix} + \begin{bmatrix} t_x \\ t_y \\ t_z \end{bmatrix} \quad (1)$$

$$R = \begin{bmatrix} \cos\varphi\cos\kappa & \cos\omega\sin\kappa + \sin\omega\sin\varphi\cos\kappa & \sin\omega\sin\kappa - \cos\omega\sin\varphi\cos\kappa \\ -\cos\varphi\sin\kappa & \cos\omega\cos\kappa - \sin\omega\sin\varphi\sin\kappa & \sin\omega\cos\kappa + \cos\omega\sin\varphi\sin\kappa \\ \sin\varphi & -\sin\omega\cos\varphi & \cos\omega\cos\varphi \end{bmatrix} \quad (2)$$

Where **R** (ω,φ,κ) is the orthogonal rotation matrix (Equation 2), $t_x$, $t_y$, $t_z$ are the elements of the translation vector and c is the scale factor. Since the functional model is non-linear, it is solved using an iterative least-squares adjustment.

To perform least squares estimation, Equation 1 must be linearized by Taylor expansion (regarding the 7 parameters: $t_x$, $t_y$, $t_z$, c, ω, φ, κ), creating the Equation 3, in matrix notation.

Using the stochastic Gauss Markov model, related to a linear combination of the parameters, the observations are assumed as non-correlated. Having a standard deviation of $\sigma = \pm 0.05$m, the solution of Equation 3 is produced by the Equation 4. In Equation 4, **W** is the diagonal weight matrix of the observations, while the best estimation of the vector $\hat{\mathbf{X}}$ of the parameters is given by Equation 5. As an illustration, in Figure 4 the surface patch of the control surface P can be defined by 3 points ($p_m$,$p_k$,$p_\ell$) and one point of Q point cloud has to be transformed to the closer surface patch. Let the projection of $q_i$ ($x_{qi}$, $y_{qi}$, $z_{qi}$) point to the surface patch be the $q_i'$ ($x_{qi}'$, $y_{qi}'$, $z_{qi}'$).

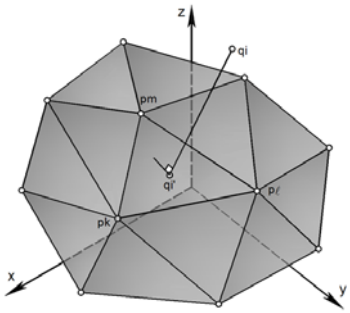


**Figure 4.** Point $q_i$ is a point of surface Q that is transformed to surface patch of P surface as $q_i'$. The shortest distance from $q_i$ to the surface is used for determining the 3D transformation

$$\mathbf{A}\delta\mathbf{x} = \delta\ell + \mathbf{v} \tag{3}$$

$$\delta\mathbf{x} = \left(\mathbf{A}^{\mathrm{T}}\mathbf{W}\mathbf{A}\right)^{-1}\mathbf{A}^{\mathrm{T}}\mathbf{W}\delta\ell \tag{4}$$

$$\hat{\mathbf{x}} = \mathbf{x}^{\mathrm{o}} + \boldsymbol{\delta}\mathbf{x} \tag{5}$$

Where, **A** is the design matrix, which includes as many rows as the number of observation equations that are created corresponding to the number of points in Q point cloud and as many columns as the number of parameters, namely equal to 7. Moreover, $\boldsymbol{\delta}\mathbf{x}$ is the vector of the corrections of the approximation values $\mathbf{x}^{\mathrm{o}}$ of the unknown parameter vector **x**, $\boldsymbol{\delta}\ell = \ell - \ell^{\mathrm{o}}$ is the second part of the observation equation and **v** the residual vector. The vector $\boldsymbol{\delta}\ell$ is calculated by the subtraction of the right part from the left part of Equation 1 using the approximation values $\mathbf{x}^{\mathbf{o}}$.

Parameters of plane's equation, which is passed from the 3 known points ($p_m$,$p_k$,$p_\ell$), are given by the 4 derivatives in Equation 6.

$$\begin{aligned} A &= \begin{vmatrix} y_{pm} & z_{pm} & 1 \\ y_{pk} & z_{pk} & 1 \\ y_{p\ell} & z_{p\ell} & 1 \end{vmatrix} \qquad B = \begin{vmatrix} x_{pm} & z_{pm} & 1 \\ x_{pk} & z_{pk} & 1 \\ x_{p\ell} & z_{p\ell} & 1 \end{vmatrix} \\ C &= \begin{vmatrix} x_{pm} & y_{pm} & 1 \\ x_{pk} & y_{pk} & 1 \\ x_{p\ell} & y_{p\ell} & 1 \end{vmatrix} \qquad D = \begin{vmatrix} x_{pm} & y_{pm} & z_{pm} \\ x_{pk} & y_{pk} & z_{pk} \\ x_{p\ell} & y_{p\ell} & z_{p\ell} \end{vmatrix} \end{aligned} \tag{6}$$

Based on Equation 6 coordinates of $q_i'$ ($x_{qi}'$, $y_{qi}'$, $z_{qi}'$), projection of $q_i$ ($x_{qi}$, $y_{qi}$, $z_{qi}$) point on the plane ($p_m$,$p_k$,$p_\ell$), are given by the Equation 7.

$$\begin{aligned} x_{qi'} &= x_{qi} - \frac{Ax_{qi} - By_{qi} + Cz_{qi} - D}{A^2 + B^2 + C^2}A \\ y_{qi'} &= y_{qi} + \frac{Ax_{qi} - By_{qi} + Cz_{qi} - D}{A^2 + B^2 + C^2}B \\ z_{qi'} &= z_{qi} - \frac{Ax_{qi} - By_{qi} + Cz_{qi} - D}{A^2 + B^2 + C^2}C \end{aligned} \tag{7}$$

As this is a non-linear problem it is clear that for the first iteration initial approximation values for the unknown parameters $\mathbf{x}^{\mathrm{o}}$ are needed. The initial approximation values of the unknown parameters had been set equal to zero (0) i.e. for the rotations and the translations. As alternative a known matching method from the literature, (e.g. Habib and Schenk, 1999) is suggested.

### 3.2 Mathematical Model of Algorithm B

An extended algorithm B has been developed in order to improve the registration. In this approach the calculation of the transformation is applied providing coordinates of $q_{i'}$ point by the already transformed point, in the P surface, instead of the initial point $q_i$ as was done in the A algorithm. As a result, coordinates of $q_{i'}$ point are represented as a function of the 7 transformation parameters. Therefore, Equation 7 should be converted to Equation 8. In matrix notation, Equation 9 can represent the whole system. After the system having taken this shape one can realize that in the observation equation the plane's parameters are also included.

$$\begin{aligned} x_{qi'} &= x_{qi} - \frac{AAx_{qi}}{A^2+B^2+C^2} + \frac{BAy_{qi}}{A^2+B^2+C^2} - \frac{CAz_{qi}}{A^2+B^2+C^2} + \frac{DA}{A^2+B^2+C^2} \\ y_{qi'} &= y_{qi} + \frac{ABx_{qi}}{A^2+B^2+C^2} - \frac{BBy_{qi}}{A^2+B^2+C^2} + \frac{CBz_{qi}}{A^2+B^2+C^2} - \frac{DB}{A^2+B^2+C^2} \\ z_{qi'} &= z_{qi} - \frac{ACx_{qi}}{A^2+B^2+C^2} + \frac{BCy_{qi}}{A^2+B^2+C^2} - \frac{CCz_{qi}}{A^2+B^2+C^2} + \frac{DC}{A^2+B^2+C^2} \end{aligned} \tag{8}$$

Equation 9 is produced by importing Equation 1 to Equation 8. Where **T** is represented the symmetrical transformation matrix of x, y, z and **L** is the matrix of constant values. In order to make the distance $q_i$-$q_{i'}$ equal to zero, Equation 9 should satisfy Equation 1, for any $q_i$ point, according to Equation 10. This Equation 10 is the new observation equation for any point. It must be linearized by Taylor expansion (regarding the 7 parameters: $t_x$, $t_y$, $t_z$, c, ω, φ, κ) while $\ell = \mathbf{0}$ and $\ell^{\mathrm{o}}$ is the result of Equation 10 using approximation values of 7 parameters.

$$\begin{bmatrix} x_{qi'} \\ y_{qi'} \\ z_{qi'} \end{bmatrix} = \mathbf{T}\cdot\left(c\cdot\mathbf{R}\cdot\begin{bmatrix} x_{qi} \\ y_{qi} \\ z_{qi} \end{bmatrix} + \begin{bmatrix} t_x \\ t_y \\ t_z \end{bmatrix}\right) + \mathbf{L} \tag{9}$$

$$\begin{aligned} &T\cdot\left(c\cdot R\cdot\begin{bmatrix} x_{qi} \\ y_{qi} \\ z_{qi} \end{bmatrix} + \begin{bmatrix} t_x \\ t_y \\ t_z \end{bmatrix}\right) + L - c\cdot R\cdot\begin{bmatrix} x_{qi} \\ y_{qi} \\ z_{qi} \end{bmatrix} - \begin{bmatrix} t_x \\ t_y \\ t_z \end{bmatrix} = 0 \Leftrightarrow \\ &(T-I)\cdot\left(c\cdot R\cdot\begin{bmatrix} x_{qi} \\ y_{qi} \\ z_{qi} \end{bmatrix} + \begin{bmatrix} t_x \\ t_y \\ t_z \end{bmatrix}\right) + L = 0 \end{aligned} \tag{10}$$

From Equations 9 and 10 one can see that both are functions of **T** and **L** matrixes. Therefore, they depend on the surface, which approximates the points. In this research the plane was this

surface. With the same methodology corresponding equations can be achieved also for different kinds of surfaces.

## 4. EXPERIMENTS AND RESULTS

The test area is a part of a city that consists of buildings, trees, bare ground, and paved roads. The evaluation has the intention to test the algorithms in these real conditions. The test area which is depicted in Figure 5, covers 2000m$^2$ approximately.
The surface P generated by photogrammetric means was chosen as the control reference system, while the surface Q generated by the laser scanning was registered allowing the surfaces to be transformed to a common reference system. The results of the tests performed creating TINs by photogrammetric points are presented in Table 1 (Projects 1-4).

**Figure 5.** Image coverage of the test area

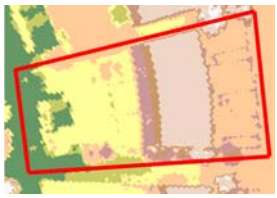

**Figure 6.** Interpolated LiDAR points

It has to be noted that in this research LiDAR points were not interpolated in any step. In Figure 6 interpolated LiDAR points are presented only for the visualization.
While the number of the laser points in this area is 27871 and it remains constant, the number of photogrammetric points was operational assisted. Both algorithms tested. In the Tables below the Abs Mean value of residuals (mm) on the algorithm A and on the algorithm B are presented. In Figure 7 one can see a project after the convergence.

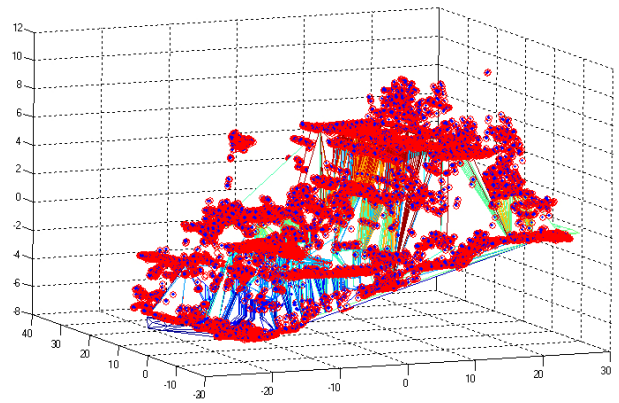

**Figure 7.** Photogrammetric restitution (highlighted TINs), LiDAR points are shown by blue circles (before) and by red circles (after the convergence) (e.g. Project 2)

Several projects were put into practice. Values of densification level of data points through a linear interpolation and the movement are also referred to the Table 2. To be more clarified, this small movement of 1mm was applied by moving the points with the lower z value outwards (e.g. the lower edge of a wall on a building).
In order to avoid arithmetic problems, due to the necessary number of digits of the coordinates, all points in both datasets (P and Q) were referred to the common Gravity Center of the two point clouds, according to numerical analysis rules.
In the Table 2 points evaluated by restitution have been interpolated by 20cm, 30cm, 40cm, 50cm respectively, in order to assess one more comparison between algorithms.
In both Tables the number of TINs is inversely proportionate to the value of the interpolation as the number of photogrammetric points is reduced while the Interpolation distance is increased. The a posteriori uncertainties of the unknown parameters are in the following range: 1μm – 9μm for $\hat{\sigma}_{tx}$, $\hat{\sigma}_{ty}$, $\hat{\sigma}_{tz}$, 0.1ppm – 3ppm for scale and 0.06$^{cc}$ – 5$^{cc}$ for $\hat{\sigma}_{t\omega}$ $\hat{\sigma}_{t\varphi}$ $\hat{\sigma}_{t\kappa}$. The above values depend on the processing level of points. In the algorithm B these values are steadily in the lower level of the above ranges. The iteration stops if every element of the vector $\hat{\mathbf{X}}$ in Equation 5 falls below a certain limit. Both algorithms converge after two iterations but the algorithm B gives slightly better results. However it is impressive that the necessary time for the convergence in the algorithm B is 50% faster.

| Project | Processing Level of Data Derived by Photogrammetric means | # of TINs |
|---|---|---|
| 1 | Breakline Interpolation 20cm Movement 1mm | 13950 |
| 2 | Breakline Interpolation 20cm | 10390 |
| 3 | Without processing | 733 |
| 4 | Movement 1mm | 1353 |

| Project | # of photo points | # of Laser points | Abs Mean of residuals A algorithm | Abs Mean of residuals B algorithm |
|---|---|---|---|---|
| 1 | 8320 | 27871 | 0.93 mm | 0.92 mm |
| 2 | 8320 | 27871 | 1.28 mm | 1.27 mm |
| 3 | 1224 | 27871 | 7.07 mm | 7.04 mm |
| 4 | 1224 | 27871 | 4.56 mm | 4.54 mm |

**Table 1.** Results of Registration between LiDAR and Photogrammetric Restitution (control surface)

| Project | Processing Level of Data Derived by Photogrammetric means | # of TINs |
|---|---|---|
| 1 | Breakline Interpolation 20cm | 13950 |
| 5 | Breakline Interpolation 30cm | 9333 |
| 6 | Breakline Interpolation 40cm | 7027 |
| 7 | Breakline Interpolation 50cm | 5743 |

| Project | # of photo points | # of Laser points | Abs Mean of residuals A algorithm | Abs Mean of residuals B algorithm |
|---|---|---|---|---|
| 1 | 8320 | 27871 | 0.93 mm | 0.92 mm |
| 5 | 5724 | 27871 | 1.23 mm | 1.22 mm |
| 6 | 4437 | 27871 | 1.47 mm | 1.45 mm |
| 7 | 3699 | 27871 | 1.65 mm | 1.64 mm |

**Table 2.** Results of Registration. Different level of Linear Breakline Interpolation. Movement 1mm

## 5. CONCLUSIONS

The aim of this research was the registration of two datasets, which were produced by different methods, into a common system. The two surfaces were defined by irregularly distributed points, while the point density was different in each of them. Registration of these two surfaces is the prerequisite step for fusion. By fusing the two surfaces, the digital elevation model (DEM) provided from LiDAR is being improved.
A prototype implementation of algorithm A developed in Pothou et al., 2006a while in this paper an extended algorithm B evolved. Both algorithms applied in a widely EuroSDR dataset from Finland. The two algorithms (A and B) used for the registration are based on the minimization of the distances between surface patches of the control surface and points of the

surface which is registered, parallel to the corresponding surface normals. Two stand-alone macros, one for each algorithm, were created for the registration of two surfaces in order to evaluate their capability under real conditions. Assessing the two algorithms could be concluded that both produced identical results, moreover the extended one B was 50% faster. As far as the convergence is concerned no difference was perceived (all projects converged after two iterations) and similar values for the parameters were accomplished.

There were two processing steps of photogrammetric points: the Breakline Interpolation and the Movement. According to the results, the Interpolation produced a denser TIN model of the photogrammetric points, and the Movement by moving (1mm) the points with the lower z value outwards (e.g. the lower edge of a wall on a building) proved to be sufficient in order to overcome the 2D Delaunay's algorithm limitation creating more triangles and a more accurate TIN model.

Apart from the faster solution, the contribution of the extended algorithm is (Equations 9 and 10) that both are functions of **T** and **L** matrices. Therefore, they depend on the surface, which is approximated by the points. In this research the plane was this surface. With the same methodology corresponding equations can also be developed for different kinds of surfaces. Moreover during a future evaluation, interesting and reliable results are expected in dense, residential or rural areas.

## 6. REFERENCES


Ackermann, F. (1999). Airborne laser scanning – present status and future expectations. *ISPRS,* 54(1) pp.64-67.

Akca, D. (2004). A new algorithm for 3D surface matching. International Archives of the Photogrammetry, *ISPRS*, Turkey, vol. XXXV, part B7 pp.960-965.

Axelsson, P. (1999). Processing Of Laser Scanner Data - Algorithms And Applications, *ISPRS*, 54(2-3), pp. 138-147.

Axelsson, P. (2000). DEM Generation From Laser Scanner Data Using Adaptive TIN Models, *IAPRS,* Annapolis, MD, Vol. 33, Part B3/1, pp. 119-126.

Balis, V., S. Karamitsos, I. Kotsis, C. Liapakis and N. Simpas (2003). 3D - Laser Scanning: Integration of Point Cloud and CCD Camera Video Data for the Production of High Resolution and Precision RGB Textured Models: Archaeological Monuments Surveying Application in Ancient Ilida, *FIG 2004*, 27th General Assembly, Athens, Greece.

Baltsavias, E. (1999). A comparison between photogrammetry and laser scanning. *ISPRS,* 54(1) pp.83-94.

Besl, P.J., and McKay N.D. (1992). A method for registration of 3D shapes. IEEE Trans. on Pattern Analysis and Machine Intelligence, 14 (2) pp.239-256.

Burman, H. (2000). Adjustment of laserscanner data for correction of orientation errors. *IAPRS*, Vol. XXXIII-3/W4, Part B3/1 pp.125-132.

Csathó, B., T. Schenk, D.C. Lee, and S. Filin (1999). Inclusion of multispectral data into object recognition. *IAPRS,* Valladolid, Spain, Vol. XXXII, Part 7-4-3W6, 8 pages.

Ebner, H., and F. Mueller (1986). Processing of Digital Three Line Imagery using a generalized model for combined point determination. *IAPRS,* 26(3/1) pp.212-222.

Ebner, H., and G. Strunz (1988). Combined point determination using Digital Terrain Models as control information. *IAPRS*, 27(B11/3) pp.578-587.

Gruen, A. (1985). Adaptive least squares correlation: a powerful image matching technique. *South African Journal of Photogrammetry, Remote Sensing and Cartography*, 14(3) pp.175-187.

Gruen, A., and D. Akca (2004). Least Squares 3D Surface Matching. *IAPRS,* Remote Sensing and Spatial Information Sciences, *"Panoramic Photogrammetry Workshop",* Dresden, Germany, vol. XXXIV, part 5/W16 (on CD-ROM).

Habib, A., and T. Schenk (1999). A new approach for matching surfaces from laser scanners and optical sensors. *IAPRS*, 32(3-W14) pp.55–61.

Kaartinen, H., J. Hyyppä, E. Gülch, H. Hyyppä, L. Matikainen, G. Vosselman, A.D. Hofmann, U. Mäder, Å. Persson, U. Söderman, M. Elmqvist, A. Ruiz, M. Dragoja, D. Flamanc, G. Maillet, T. Kersten, J. Carl, R. Hau, E. Wild, L. Frederiksen, J. Holmgaard, and K. Vester (2005). EuroSDR Building Extraction Comparison. *ISPRS Hannover Workshop "High-Resolution Earth Imaging for Geospatial Information",* May 17-20, CD-ROM, 6 p.

Kraus, K., Pfeifer, N. (1998). Determination Of Terrain Models In Wooded Areas With Airborne Laser Scanner Data, *ISPRS*, Vol. 53, pp. 193-203.

Maas, H.G. (2000). Least-Squares Matching with airborne laserscanning data in a TIN structure. *IAPRS,* 33(3A)

Morgan, M., and A. Habib (2002). Interpolation of LiDAR Data and Automatic Building Extraction. *ASPRS,* Washington.

Morgan, M., and A. Habib (2001). 3D TIN for Automatic Building Extraction from Airborne Laser Scanning Data. *ASPRS,* St. Louis, Missouri.

Paska, E. and Toth, C., (2003), LIDAR Data Segmentation Based on Morphologic Filtering, *ASPRS*, May 5-9, Anchorage, Alaska, CD-ROM.

Postolov, Y., A. Krupnik, and K. McIntosh (1999). Registration of airborne laser data to surfaces generated by Photogrammetric means. *IAPRS*, 32(3/W14) pp.95-99.

Pothou A., S. Karamitsos, A. Georgopoulos and I. Kotsis (2006a). Performance evaluation for aerial images and airborne Laser Altimerty dara registration procedures. *ASPRS,* Nevada.

Schenk, T., A. Krupnik, and Y. Postolov (2000). Registration of airborne laser data to surfaces generated by Photogrammetric means. *IAPRS*, 32(3/W14) pp.95-99.

Toth, C., and D. Grejner-Brzezinska (1999). Improved DEM extraction techniques - combining LIDAR data with direct digital GPS/INS orientated imagery. *International Workshop on Mobile Mapping Technology*, Bangkok, Thailand.

Vosselman, G. (1999). Building reconstruction using planar faces in very high density height data. *IAPRS,* Vol. XXXII, Part 3-2W5 pp.87-92.

Vosselman, G. (2000). Slope Based Filtering Of Laser Altimetry Data, *IAPRS,* Annapolis, MD, Vol. 33, Part B3/2.


## 7. ACKNOWLEDGEMENTS


We are grateful to Finnish Geodetic Institute, Masala, Finland and in particular to Harri Kaartinen for providing the data set.